Kinetic Characterization of the Serralysins: A Divergent Catalytic Mechanism Pertaining to Astacin-Type Metalloproteases†

William L. Mock* and Jun Yao

Department of Chemistry, University of Illinois at Chicago, Chicago, Illinois 60607-7061

Received December 27, 1996⊗

ABSTRACT: Substrates $HO_2CCH_2CH_2CO$- and $HOCH_2CHOHCHOHCO$-Phe-Leu-Ala-5-nitro-2-pyridinamide are cleaved efficiently at the acylarenamide linkage, with a convenient spectrophotometric assay, by the *Serratia* and *Pseudomonas* ∼50-kDa extracellular metalloproteases (serralysins). The pH range of catalytic activity extends uniformly from 4 to greater than 10 (k_{cat}/K_m $\sim 10^3$ s^{-1} M^{-1}, similar profile for k_{cat}). Substrate analogue hydroxamic acid Cbz-Leu-Ala-NHOH competitively inhibits serralysin (K_i 0.04 mM), with a pH dependence indicating that either a displaced metal-bound H_2O or a similarly motile enzymic phenol residue (Tyr 216) that is crystallographically found ligated to the active-site Zn^{2+} of the uncomplexed enzyme must have a pK_a of ∼5. A chemical catalytic mechanism of proteolysis consistent with the kinetic data is proposed, in which Tyr 216-ArO^-, in the course of being released from the active-site metal ion, deprotonates a water molecule attacking the Zn^{2+}-activated substrate linkage, leading to a metal-coordinated tetrahedral oxyanion adduct that subsequently fragments.

The important question of chemical mechanism for the zinc proteases continues to draw attention (Mock & Stanford, 1996). A 50-kDa metalloprotease (SMP)[1] that is excreted into the culture medium by *Serratia marcescens* is representative of a collection of bacterially produced homologous enzymes (serralysin family; Jiang & Bond, 1992; Hooper, 1994; Stöcker et al., 1995; Rawlings & Barrett, 1995). The latter includes similar proteases from *Pseudomonas* and from *Erwinia*. These enzymes also appear to fall within a superfamily known as the metzincins, with the latter including the snake venom proteases and collagen-matrix cleaving proteases related to astacin, the prototypical member (Stöcker & Bode, 1995; Bond & Beynon, 1995). The serralysins differ from the better-studied group of enzymes represented by the metalloendoprotease thermolysin in that they exploit three histidine residues plus a tyrosine for holding the Zn^{2+} ion at the active site instead of two histidines and a glutamic acid residue. Other active-site features are sufficiently different in the two groups of enzymes to suggest that thorough kinetic investigation is desirable for the serralysins and would be beneficial as regards mechanistic understanding for the entire class of metalloproteases.

MATERIALS AND METHODS

Enzyme and Buffer Solutions Employed. The parent enzyme serralysin (SMP) was supplied by Sigma Chemical Co., no. P 2789, lot 76F014, and was shown to contain >95% of a single protein (∼50 kDa) by SDS−polyacrylamide gel electrophoresis, after aqueous incubation with phenanthroline to inhibit autodigestion during analysis. The enzyme employed for kinetics is the same as that upon which crystallographic structure determinations have been carried out. Protein content was estimated from nitrogen elemental analysis and the known amino acid composition of the enzyme. Alkaline protease (AP, from *Pseudomonas aeruginosa*) was supplied by Nagase Biochemicals Ltd., lot 6349089, and was of certified purity. Buffers employed in this work for kinetic analysis (0.02 M each) were as follows: pH 3.6-5.1, iminodipropionitrile; pH 4.3-5, piperazine; pH 5−6.5, 2-(*N*-morpholino)ethanesulfonic acid; pH 6.9−8, *N*-(2-hydroxyethyl)piperazine-*N*′-(2-ethanesulfonic acid); pH 8.4−10, 2-(*N*-cyclohexylamino)ethanesulfonic acid; pH 10.5, 3-(cyclohexylamino)-1-propanesulfonic acid. All were shown to give negligible kinetic perturbations with serralysin.

Preparation of Boc-Ala-NH(C_5H_3N)NO_2. A solution of 5.00 g (17.5 mmol) of *N*-(*tert*-butoxycarbonyl)-L-alanine *N*-hydroxysuccinimide ester (Sigma no. B 2130) and 2.53 g (18.2 mmol) of 5-nitro-2-pyridinamine (Acros no. 10423) in 5 mL of dimethylformamide containing 3 drops of triethylamine was heated at 85−90 °C for 18 h (the reaction appears to reach an equilibrium short of completion). The resulting solution was diluted with 320 mL of ethyl acetate and was extracted (×2) with 200 mL of 0.1 N hydrochloric acid, with 0.01 N sodium hydroxide until the washings were pH 7, then with water, and finally with saturated sodium chloride. Rotary evaporation of the ethyl acetate gave an oil, which was taken up in chloroform and diluted to the cloud point with hexane. Upon standing, a precipitate of product plus unreacted nitropyridinamine formed and was collected. It was purified by silica chromatography (EtOAc−hexanes 1:2). The desired material was recrystallized from chloroform and carbon tetrachloride, giving 2.17 g (40%) of *N*-(*tert*-butoxycarbonyl)-L-alanyl-5-nitro-2-pyridinamide, mp 158−158.5 °C; IR (KBr) 1680 cm^{-1}; ^1H 400-MHz NMR ($CDCl_3$) δ 1.48 (s, 9 H), 1.49 (d, 3 H, J = 8 Hz), 4.45 (br,

† This work was supported by NIH Grant GM39740.

* Corresponding author. FAX: 312-996-0431. E-mail: wlmock@uic.edu.

⊗ Abstract published in *Advance ACS Abstracts,* April 1, 1997.

[1] Abbreviations: Txl (L-threoxyl), threonic (2*R*,3*S*-2,3,4-trihydroxybutanoic) acid residue; Suc, succinyl residue; SMP, *Serratia (marcescens)* metalloprotease; AP, alkaline protease from *Pseudomonas aeruginosa*. The designations used for the amino acid residues (P) of the substrate and to name the subsites (S) of the enzymic active site are those of Schechter and Berger (1967).

S0006-2960(96)03149-2 CCC: $14.00

1 H), 5.13 (br, 1 H), 8.40 (d, 1 H $J = 9.2$), 8.49 (dd, 1 H, $J = 2.4$ and 9.2 Hz), and 9.15 (d, 1 H, $J = 2.4$ Hz); UV (H_2O) 307 nm (ϵ 10 300); $[\alpha]_D^{28} = -18.9°$ (Me_2CO, $c = 0.19$).

Preparation of (H)Ala-NH(C_5H_3N)NO_2·HCl. To a solution of 4.21 g (13.6 mmol) of *N*-(*tert*-butoxycarbonyl)-L-alanyl-5-nitro-2-pyridinamide in 70 mL of ethyl acetate in an ice bath was added a saturated solution of anhydrous hydrogen chloride in 100 mL of ethyl acetate. After 30 min at room temperature a white precipitate had formed, which was collected and washed with a small amount of ethyl acetate. The resulting powder was evacuated in a desiccator over potassium hydroxide pellets for 2 h. The product was dissolved in methanol and precipitated with diethyl ether, yielding 2.10 g (63%) of L-alanyl-5-nitro-2-pyridinamide hydrochloride, mp ~115 °C (foam/dec).

Preparation of (H)Phe-Leu-Ala-NH(C_5H_3N)NO_2·HBr. To a mixture of 3.41 g (8.3 mmol) of *N*-carbobenzyloxy-L-phenylalanyl-L-leucine (Sigma no. C 1141), 2.04 g (8.3 mmol) of L-alanyl-5-nitro-2-pyridinamide hydrochloride, 1.12 g (8.3 mmol) of 1-hydroxybenzotriazole, and 0.84 g (8.3 mmol) of triethylamine in 40 mL of dimethylformamide was added 4.01 g (9.5 mmol) of 1-cyclohexyl-3-(2-morpholinoethyl)carbodiimide metho-*p*-toluenesulfonate, and the resulting homogeneous solution was allowed to stand overnight at 25 °C. The resulting solution was poured into 300 mL of a mixture of ice and water to precipitate the product, which was collected. The solid was redissolved in dimethylformamide and again poured into water. The precipitate was dried and recrystallized from 100 mL of hot glacial acetic acid. Additional material was secured from the filtrate by addition of diethyl ether. Obtained was 3.49 g (70%) of *N*-carbobenzyloxy-L-phenylalanyl-L-leucyl-L-alanyl-5-nitro-2-pyridinamide, mp 244−245 °C.

A solution of 3.49 g (5.8 mmol) of *N*-carbobenzyloxy-L-phenylalanyl-L-leucyl-L-alanyl-5-nitro-2-pyridinamide in 45 g of 30% hydrogen bromide in acetic acid was allowed to stand at 25 °C for 0.5 h. Subsequent dilution with 600 mL of anhydrous diethyl ether gave a suspension that was allowed to stand for 0.5 h on crushed ice. The resulting solid was collected and was promptly desiccated over potassium hydroxide pellets for 2 h. The product was recrystallized by dissolution in 150 mL of methanol with subsequent dilution by 300 mL of anhydrous diethyl ether, followed by standing at 0−5 °C. The solid was collected and dried, giving 2.39 g (75%) of L-phenylalanyl-L-leucyl-L-alanyl-5-nitro-2-pyridinamide hydrobromide, mp 268−269 °C (dec); UV (H_2O) 308 nm (ϵ 14 400).

Preparation of Txl-Phe-Leu-Ala-NH(C_5H_3N)NO_2. To a solution of 4.45 g (8.1 mmol) of L-phenylalanyl-L-leucyl-L-alanyl-5-nitro-2-pyridinamide hydrobromide, 1.58 g (8.1 mmol) of 3,4-*O*-isopropylidene-L-threonic acid calcium salt (Aldrich no. 38,065-2) and 1.09 g (8.1 mmol) of 1-hydroxybenzotriazole in 50 mL of dimethylformamide was added 3.90 g (9.2 mmol) of 1-cyclohexyl-3-(2-morpholinoethyl)-carbodiimide metho-*p*-toluenesulfonate, and the solution was allowed to stir overnight at 25 °C. The resulting solution was poured into 500 mL of ice and water, and a solid was collected. The product was recrystallized by dissolving in methanol and reprecipitating with water, yielding 4.10 g (81%) of *N*-(3,4-*O*-isopropylidene-L-threoxyl)-L-phenylalanyl-L-leucyl-L-alanyl-5-nitro-2-pyridinamide, mp 174.5−175.5 °C.

Into a solution of 4.04 g (6.4 mmol) of *N*-(3,4-*O*-isopropylidene-L-threoxyl)-L-phenylalanyl-L-leucyl-L-alanyl-5-nitro-2-pyridinamide in 100 mL of methanol was added dropwise 10 mL of 6 N hydrochloric acid at 25 °C. The reaction mixture was stirred for 1 h and was then neutralized with aqueous ammonia to a pH of 6. The methanol was rotary-evaporated and the product was precipitated with 20 mL of water. The solid was collected and washed with 10 mL of cold water. It was then triturated with warm ethyl acetate, giving 3.40 g (90%) of *N*-L-threoxyl-L-phenylalanyl-L-leucyl-L-alanyl-5-nitro-2-pyridinamide, mp 191.5−192.5 °C; UV (MeOH) 307 nm (ϵ 15 400); IR (KBr) 3360, 1725, and 1640 cm^{-1}; ^1H 400-MHz NMR (CD_3SOCD_3) δ 0.85 (dd, 6 H, $J = 6.4$ and 13.8 Hz), 1.34 (d, 3 H, $J = 7.2$ Hz), 1.45 (m, 2 H), 1.54 (m, 1 H), 2.97 (m, 1 H), 3.04 (m, 1 H), 3.37 (m, 2 H), 3.71 (m, 1 H), 3.93 (m, 1 H), 4.40 (m, 1 H), 4.52 (m, 2 H), 4.58 (m, 1 H), 4.70 (d, 1 H, $J = 6.1$ Hz), 5.49 (d, 1H, $J = 6.5$ Hz), 7.16−7.26 (m, 5 H), 7.73 (d, 1 H, $J = 8.1$ Hz), 7.98 (d, 1 H, $J = 8.6$ Hz), 8.25 (m, 2 H), 8.59 (dd, 1 H, $J = 2.9$ and 9.4 Hz), 9.17 (d, 1 H, $J = 2.7$ Hz), and 11.27 (s, 1 H). Anal. Calcd for $C_{27}H_{36}O_9N_6$: C 55.09, H 6.16, N 14.28. Found: C 55.26, H 6.45, N 14.04.

Preparation of Suc-Phe-Leu-Ala-NH(C_5H_3N)NO_2. To a suspension of 2.36 g (4.28 mmol) of L-phenylalanyl-L-leucyl-L-alanyl-5-nitro-2-pyridinamide hydrobromide and 0.433 g (4.28 mmol) of triethylamine 40 mL of acetonitrile was added 0.428 g (4.28 mmol) of succinic anhydride (freshly recrystallized from $CHCl_3$). The mixture was swirled for 5 min until all particles of the hydrobromide dissolved, and the resulting cloudy solution was allowed to stand at 25 °C for 1 h. The acetonitrile was then rotary-evaporated and the residue was partitioned between 800 mL of ethyl acetate and 400 mL of 1 N hydrochloric acid. The organic phase was washed with saturated sodium chloride, and then was rotary evaporated to a volume of ~100 mL (cloudy solution). After standing, the resulting white precipitate was collected, washed with hexane, and allowed to air-dry, giving 2.17 g (89%) of *N*-succinyl-L-phenylalanyl-L-leucyl-L-alanyl-5-nitro-2-pyridinamide as a white powder, mp 228−229 °C; UV (H_2O, phosphate buffer) pH < 9.5, 308 nm (ϵ 13 900), pH > 12.5, 353 nm (ϵ 12 500), $pK_a = 11.1$ (±0.1); IR (KBr) 1700 and 1620−1660 cm^{-1}; ^1H 400−MHz NMR (CD_3SOCD_3) similar to Txl derivative (with replacement of threoxyl signals by those of succinyl residue). Anal. Calcd for $C_{27}H_{34}N_6O_8$: C 56.83, H 6.01, N 14.73. Found: C 56.40, H 6.19, N 14.39.

Preparation of Cbz-Leu-Ala-NHOH. A solution of 1.75 g (5.2 mmol) of *N*-carbobenzyloxy-L-leucyl-L-alanine (Sigma no. C 0170) in 3 mL of dimethylformamide was added to a solution of 1.07 g (5.2 mmol) of 1,3-dicyclohexylcarbodiimide in 4 mL of dimethylformamide in an ice bath. A solution of 0.60 g (5.2 mmol) of *N*-hydroxysuccinimide in 2 mL of dimethylformamide was immediately added to the above mixture. The solution was stirred in an ice bath for 2 h, and the mixture was then stirred at room temperature overnight. The white precipitate that formed was removed by filtration. The filtrate was poured into 100 mL of cool water to precipitate the product, which was collected. The resulting solid was recrystallized from chloroform−carbon tetrachloride, giving 2.00 g (89%) of *N*-carbobenzyloxy-L-leucyl-L-alanyl-*N*-hydroxysuccinimide as white crystals, mp 163−164 °C; IR (KBr) 1810, 1780, 1750, 1685, and 1650 cm^{-1}.

To a mixture of 1.90 g (4.4 mmol) of *N*-carbobenzyloxy-L-leucyl-L-alanyl-*N*-hydroxysuccinimide and 3.0 g (43.2 mmol) of hydroxylamine hydrochloride in 100 mL of methanol−chloroform (1:1) in an ice bath was added 17.3 g of 10% sodium hydroxide solution. The resulting mixture was stirred for 2 h in an ice bath. A precipitate was removed by filtration, and the solution was evaporated. The residue was dissolved in 50 mL of ethyl acetate and was extracted with 50 mL of 0.1 N hydrochloric acid and then with saturated sodium chloride. The ethyl acetate was rotary-evaporated to a volume of 10 mL and was then diluted to the cloud point with hexanes. A solid was collected by filtration, 1.20 g (78%) of *N*-carbobenzyloxy-L-leucyl-L-alanyl-*N*-hydroxylamide, mp 158−158.5 °C; IR (KBr) 1640 and 1690 cm^{-1}; ^1H 200-MHz NMR (CD_3SOCD_3) δ 0.85 (dd, 6 H), 1.15 (d, 2 H), 1.35−1.60 (m, 2 H), 3.98−4.20 (m, 2 H), 5.00 (s, 2 H), 7.28−7.42 (m, 6 H), 7.95 (d, 1 H), 8.86 (s, 1 H), and 10.58 (s, 1 H). Anal. Calcd for $C_{17}H_{25}N_3O_5$: C 58.11, H 7.17, N 11.96. Found: C 58.03, H 7.31, N 11.71. A UV spectrophotometric titration of this material (245 nm, buffer 10 mM 1,3-propanediamine) gave a pK_a value of 9.1 (±0.1) for ionization of the hydroxamic acid.

Crystal Structure Determination, SMP·I Complex. The adduct between serralysin and Cbz-Leu-Ala-NHOH has been examined by Ulrich Baumann of the Biomolecular Structure Unit, Institute of Cancer Research, Sutton SM2 5NG, U.K., and a portion of its structure is described here with permission, with full details to be published separately. The *Serratia* protease was crystallized as described previously (Baumann, 1994). Crystals having a typical size of 0.2 × 0.4 × 0.6 mm were grown at 4 °C and were soaked for 48 h in a solution containing 10 mM Cbz-Leu-Ala-NHOH. Data were collected on a MAR research image plate at a crystal-to-plate distance of 110 mm. Data were processed using DENZO/SCALEPACK; relevant statistics are tabulated below. Difference Fourier maps revealed the presence of the inhibitor in the active-site cleft. Refinement was carried out using X-plor, applying a bulk solvent mask and an anisotropic overall *B*-factor correction in the last rounds of refinement.

resolution	1.80 Å
no. of measured/unique relections	238 329/61 944
$R(I)$	0.058
completeness	0.934

Cbz-Leu-Ala-NHOH binds to SMP in a fashion similar to peptides found in the crystal structure of AP (Baumann et al., 1993). The Leu-Ala backbone of the inhibitor binds in an extended manner, antiparallel to an edge strand (residues 133−137) of β-sheet, forming two backbone H-bonds with residue Ala 136, while the side chain of Asn 191 on the other side of the active-site cleft H-bonds to the alanyl nitrogen of the inhibitor. The carbobenzyloxy group does not have significant electron density and is probably disordered. Features of the active-site Zn^{2+} ligation are presented in a subsequent figure. The complete structure has been deposited in the Brookhaven Protein Data Bank (code 1af0).

Kinetic Analysis. The catalytic pH−rate dependences (k_{cat}/K_m with [S] < K_m and where feasible k_{cat} and K_m) for the peptidyl nitropyridinamide substrates with serralysins, including inhibitor K_i data, were determined at 25.0 (±0.1) °C in buffers previously listed (containing 4% dimethyl sulfoxide and 1 mM calcium chloride), with spectrophotometric monitoring (of absorption increase at 350−400 nm, 1 or 2 cm path length) and the method of initial rates. Enzyme concentration was maintained well below substrate concentration for kinetic parameter determinations in all cases, and irreversible decay of enzyme activity was shown to be negligible over the time period of kinetic-assay runs, at the pH extremes. Ordinarily, kinetic runs were initiated by addition of enzyme to a preequilibrated solution of substrate in buffer, but for pH values of <6 with SMP the enzyme showed spontaneous activation during the initial few minutes of exposure to acid, so that an inverse mode of addition (substrate to equilibrated enzyme) had to be employed. The limiting kinetic parameters were obtained as a function of pH by a nonlinear least-squares fit of data (Michaelis parameters, similarly obtained) to the appropriate equations as given in the figure legends. All pH values in this paper are calibrated pH meter readings uncorrected for ionic strength effects. Tolerances listed are standard errors from least-squares analysis.

RESULTS

Design of an Assay Substrate. The *Serratia marcescens* protease (SMP) obtained from strain E-15 has been known for some time (Miyata et al., 1970a,b). It has been sequenced (Nakahama et al., 1986), and protein crystal structures are available showing the conformation of the enzyme (Baumann, 1994; Baumann et al., 1995; Hamada et al., 1996). In spite of this wealth of structural evidence, rather little is known regarding its specificity (Miyata et al., 1970c). From the limited data available, together with that for the similar protease from *Pseudomonas aeruginosa* (Morihara, 1963; Morihara et al., 1973) and a crystal structure for the latter (Baumann et al., 1993; Miyatake et al., 1995), an informed guess could be made as to the type of peptide that might be suitable for kinetic assay. The active-site Zn^{2+} lies at the bottom and middle of a deep groove in the protein. The S_1 subsite seems relatively constricted, but the S_2 and S_3 regions of the enzyme appear designed to hold hydrophobic side chains. Additionally, a specific H-bonding network involving the backbone amide linkages of the P_1-P_3 portions for a product peptide that was fortuitously discovered so bound in the case of the *Pseudomonas* enzyme suggested that adequate specificity might reside in that half of substrates (carboxy side of scissile linkage). Pockets indicating hydrophobic S_1' and S_2' subsites (amino side of scissile linkage) also may be observed in the protein crystal structures, but these are not exploited in our current substrate design.

On the strength of the foregoing considerations, an appropriate tripeptide *p*-nitroanilide (Erlanger et al., 1961; Wolz, 1994) was tested for kinetic competence, on the *Pseudomonas* alkaline protease (AP). Attempted cleavage of Phe-Leu-Ala-$NHC_6H_4NO_2$ was only marginally successful: At pH of 7.4 a K_m value of 0.2 mM was noted, indicating suitable substrate binding, but the estimated k_{cat} value, 0.013 s^{-1}, was unsatisfactory for routine kinetic assay (J.-T. Tsay, unpublished observations). However, substitution of 5-nitro-2-pyridinamine as the N-moiety within the scissile linkage gave enzymic cleavage at a rate several orders of magnitude faster than for the *p*-nitroanilide, with even more favorable spectrophotometric characteristics for monitoring kinetics (see Figure 1). This is a nontrivial improvement, and it makes inhibition studies and determination of pH profiles

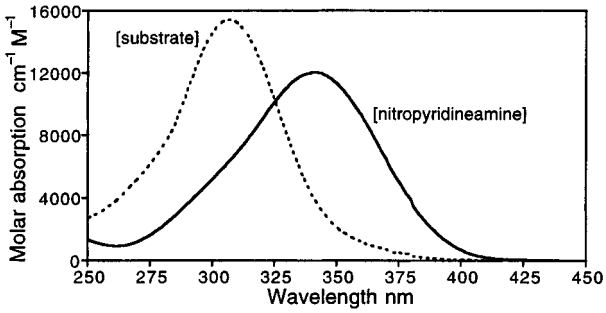

FIGURE 1: Spectral comparison of 5-nitro-2-pyridinamide substrate [Txl-Phe-Leu-Ala-NH(C_5H_3N)NO_2, dashed line] with hydrolysis product (5-nitro-2-pyridinamine, solid line), indicating the substantial absorption increase at wavelengths of >350 nm that accompanies enzymic cleavage.

Scheme 1

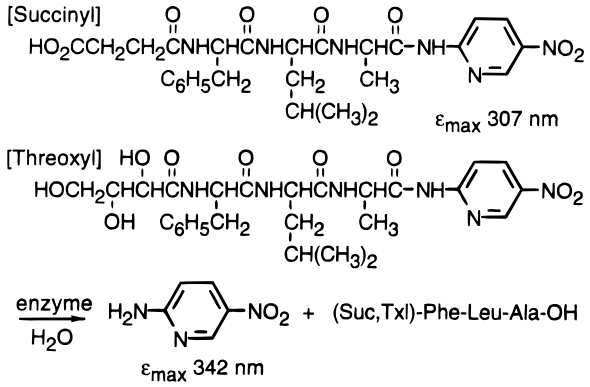

practical. However, solubility of the tripeptide was inadequate, particularly at high pH. The latter problem was solved in two ways (Scheme 1). In accord with previous practice, a succinyl residue introduced at the N-terminus was found to enhance solubility, affording Suc-Phe-Leu-Ala-NH-(C_5H_3N)NO_2 as a suitable assay substrate. However, at low pH values the introduced carboxylate becomes protonated, again causing loss of solubility and complicating kinetic assay. For an alternative end residue, a triol-containing threonic acid moiety was attached to the N-terminus of the tripeptide ($HOCH_2CHOHCHOHCO$-amide), and that hydrophilic tail conferred superior solubility to the substrate designated as Txl-Phe-Leu-Ala-NH(C_5H_3N)NO_2, at all pH values.[2] The two innovative features incorporated in the latter substrate merit special notice, namely, the scissile amide-group modification (nitropyridinamine) for assay of enzymes that are tolerant of arenamides as a leaving group in the S_1' position, plus the Txl capping residue (threoxyl) for solubilization without introduction of an anionic carboxylate into the peptide. These previously unexploited substrate components are candidates for general adoption in enzyme catalysis studies.

Catalytic Activity of SMP. With access to a convenient continuous spectrophotometric assay technique [monitoring of amide cleavage at 350−400 nm, enhancement of absorption attending release of $H_2N(C_5H_3N)NO_2$, see Figure 1] systematic investigation of the kinetic catalytic characteristics of the serralysins became feasible. Of primary importance

[2] The abbreviation Txl (threoxyl) is introduced to symbolize a threonic acid ($HOCH_2CHOHCHOHCO_2H$) residue. The latter must be clearly distinguished from the amino acid residue threonine (Thr), which is not here employed.

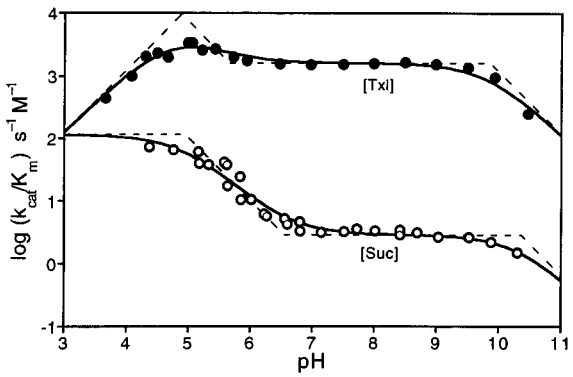

FIGURE 2: Log plot of specificity constant k_{cat}/K_m as a function of pH for cleavage of Txl-Phe-Leu-Ala-NH(C_5H_3N)NO_2 (●) and Suc-Phe-Leu-Ala-NH(C_5H_3N)NO_2 (○) by SMP. Equations for the fitted lines are $(k_{cat}/K_m)_{apparent} = (k_{cat}/K_m)_{lim}(1 + [H]/K_{a2})/\{(1 + [H]/K_{a1})^2 (1 + K_{a3}/[H])\}$ (upper) and $(k_{cat}/K_m)_{apparent} = (k_{cat}/K_m)_{lim}(1 + [H]/K_{a2})/\{(1 + [H]/K_{a1})(1 + K_{a3}/[H])\}$ (lower). Least-squares fitted parameters are as follows: Txl substrate, $(k_{cat}/K_m)_{lim} = 1600 (\pm 120)$ s^{-1} M^{-1} (value in flat region near label, pH 6−9), p$K_{a1} = 4.9 (\pm 0.1)$, p$K_{a2} = 5.6 (\pm 0.1)$, p$K_{a3} = 9.9 (\pm 0.1)$; Suc substrate, $(k_{cat}/K_m)_{lim} = 2.9 (\pm 0.3)$ s^{-1} M^{-1} (value in flat region near label, pH 7−9), p$K_{a1} = 4.9 (\pm 0.2)$, p$K_{a2} = 6.5 (\pm 0.1)$, p$K_{a3} = 10.3 (\pm 0.2)$. Breaks in dashed-line asymptotes denote pK_a values. For the Txl substrate pK_{a1} is a mean value, for two analytically unresolvable ionizations (one canceling the upstroke caused by pK_{a2}).

in this regard is the "specificity constant" k_{cat}/K_m, a second-order rate constant for conversion of substrate by enzyme under conditions of high dilution. Perturbations of this kinetic parameter are informative as to structural components of the enzyme, either influencing substrate binding or participating in the first committed step of catalysis within the E·S complex. It had previously been recognized that serralysins are active at high pH (the enzyme from *Pseudomonas* is known as "alkaline protease"). However, our nitropyridinamides allow considerably better kinetic reproducibility than has been hitherto attainable, permitting quantitative evaluation. The pH dependence for k_{cat}/K_m for the *Serratia* protease (SMP) is shown in Figure 2, for substrates Txl-Phe-Leu-Ala-NH(C_5H_3N)NO_2 and Suc-Phe-Leu-Ala-NH-(C_5H_3N)NO_2.

Velocity versus pH, [S] ≪ K_m. As may be seen, the enzyme SMP yields a remarkably broad range of activity, spanning from pH ≤3 to ≥11. The limits seem to be specified most cogently for Txl-Phe-Leu-Ala-NH(C_5H_3N)-NO_2, although there are complications on both limbs of the pH profile. For both substrates at high pH the nitropyridinamide moiety suffers nonenzymic alkaline hydrolysis, requiring corrections to the catalytic reaction. For measurement of convenient velocities, these may be carried out with confidence only for pH values of <10.5, above which the blank (hydroxide) reaction exceeds the catalytic. However, with appropriate allowance for this complication, it appears that SMP catalysis becomes suppressed in that pH range. Least-squares curve fitting to catalytic rates that have been corrected for spontaneous hydrolysis suggests a downturn in the pH profiles characterized by a pK_a of ∼10, as shown in Figure 2. This is believed to be an enzymic ionization. A pK_a value for deprotonation of the substrate chromophore has been independently measured by rapid spectrophotometric titration, and a somewhat greater pK_a value of 11.1 was found (for ionization of acylnitropyridinamide-NH). Because the kinetically observed pK_a value is significantly

lower than 11, it should be attributed to an enzyme functional group.

In the acidic region of the profile in Figure 2, SMP shows especially complicated behavior. Unlike at higher pH, maximum catalytic activity is only slowly attained when a neutral solution of the enzyme is added to a buffered acidic assay solution of either of the substrates. This suggests that some change in the enzyme is occurring, perhaps a delayed conformational shift and/or a slow protonation. For rate measurements in this pH range, an inverse assay mode was employed, in which kinetic runs were initiated by addition of substrate to an equilibrated solution of enzyme. With this provision, the small upward inflection noted in the profiles could be reproducibly examined, after a delay for the enzyme to become pH-equilibrated. With Txl-Phe-Leu-Ala-NH-(C_5H_3N)NO_2 the resulting catalytic activity becomes extinguished at lower pH values as well as in alkali. Least-squares curve fitting yields demarcating pK_a values on the acidic and alkaline limbs of 4.9 (±0.1) and 10.1 (±0.2), respectively, with a pK_a of 5.6 (±0.1) characterizing the small upward inflection within the interior of the profile. For alternate substrate Suc-Phe-Leu-Ala-NH(C_5H_3N)NO_2 the downturn on the acidic limb could not be seen. The succinyl carboxylate becomes protonated in acid with accompanying loss of substrate solubility, so the pH profile could not be extended in that case. Not surprisingly the carboxylic acid form of substrate apparently binds more tightly (K_m decreases substantially in acid, from ≥2.5 mM to ∼0.1 mM), and that accounts for the greater upward inflection in the k_{cat}/K_m profile for the Suc substrate (40-fold vs 2-fold increase) and for the absence of an eventual downturn as for the Txl substrate. Because of analytic difficulties in disentangling these phenomena for the succinylated derivative, subsequent interpretation will focus on the more active threoxyl substrate. The parent tripeptide-nitropyridinamide (that with a free terminal amino group) was also examined as a substrate and was found to be comparably active as the Txl derivative at neutral pH. It showed a diminution of activity on the acidic limb, but it could not be examined above a pH of 8 for solubility reasons. Overall, it appears that the pH range of enzymic activity for SMP is quite broad, with essentially full activity from pH 4 to 10.

Catalytic Activity of AP. The behavior of the individual Michaelis parameters k_{cat} and K_m as a function of pH is of course of interest. In the case of SMP these could not be adequately determined, since the solubility limits for our substrates (∼2.5 mM) approximates the value of K_m with that enzyme at most pH values. However, the structurally comparable metalloprotease produced by *P. aeruginosa* proved more suitable, with values for K_m of ∼0.65 mM, allowing full determination of Michaelis parameters (Figure 3). With varying pH in the case of this enzyme (AP), the specificity constant k_{cat}/K_m employing the threoxyl substrate spans essentially the same range as for SMP. Additionally, the k_{cat} vs pH profile generally parallels that of the specificity constant (i.e., K_m does not vary greatly with pH). The slight upward inflection in the acidic region seen with SMP appears to be duplicated in the k_{cat} profile, but the ultimate quenching of activity at low pH evidently is a k_{cat} phenomenon. The time-dependent activation phenomenon seen with SMP either was not present in the case of AP or was attained more quickly; hence, a "normal" experimental mode of initiating kinetic runs sufficed. On the alkaline limb of the pH profile,

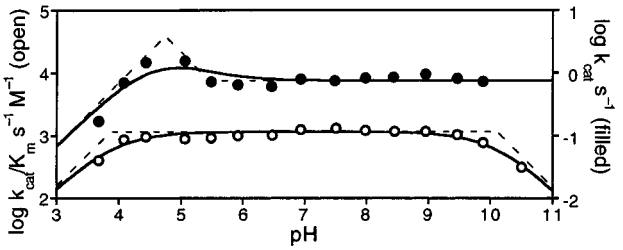

FIGURE 3: Log plot of k_{cat}/K_m (○) and of k_{cat} (●) as a function of pH for cleavage of Txl-Phe-Leu-Ala-NH(C_5H_3N)NO_2 by alkaline protease (AP). Equations for the fitted lines are $(k_{cat}/K_m)_{apparent} = (k_{cat}/K_m)_{lim}/\{(1 + [H]/K_{a1})(1 + K_{a2}/[H])\}$ (lower) and $(k_{cat})_{apparent} = (k_{cat})_{lim}(1 + [H]/K_{a2})/(1 + [H]/K_{a1})^2$ (upper). Least-squares fitted parameters are as follows: $(k_{cat}/K_m)_{lim} = 1160$ (± 50) s^{-1} M^{-1}, p$K_{a1} = 3.9$ (± 0.1), p$K_{a2} = 10.1$ (± 0.1); $(k_{cat})_{lim} = 0.75$ (± 0.08) s^{-1} (value in flat region, pH 7−9), p$K_{a1} = 4.7$ (± 0.2), p$K_{a2} = 5.5$ (± 0.3)(pK_{a1} is a mean value, as in Figure 2). Breaks in dashed-line asymptotes denote pK_a values.

a fall-off in activity for k_{cat} could not be detected for technical reasons (incipient ionization of substrate prevents suitable spectrophotometric kinetics at pH >10), so it cannot be said whether the decrease that is seen in the specificity constant there takes place within k_{cat} or within K_m.

In summary, the pH region of full activity for both SMP and AP extends from 4 to 10. This is unusual for zinc proteases: Optimal activity of the better-studied metalloproteolytic enzymes thermolysin and carboxypeptidase A is restricted to a 2−3 pH-unit range. This signals potential mechanistic differences for the serralysins.

Hydroxamate Inhibition. The key to appreciation of mechanism for thermolysin and carboxypeptidase A has been recognition of the hyper-Lewis-acidic character of the Zn^{2+} ion bound at the active site (Mock et al., 1993; Mock & Aksamawati, 1994; Mock & Stanford, 1996). The acidic-limb inflection occurring within a bell-shaped k_{cat}/K_m vs pH profile in those cases (pK_a value of 5 or 6) is in fact caused by deprotonation of a water molecule that is ligated to the tetracoordinate Zn^{2+} in the absence of substrate. The low value of that pK_a (for $H_2O{\cdot}Zn^{2+}$) constitutes a direct index of the electron deficiency of the metal ion, explaining its efficacy in stabilizing the tetrahedral-adduct oxyanion intermediate in the course of catalysis (*via* a reverse-protonation mechanism; Mock & Stanford, 1996). Whether this is also the situation in the case of the serralysins is obviously of interest. The question of Zn^{2+} Lewis acidity may be answered with the least burden of ambiguity by pH-dependent competitive inhibition evidence (Cleland, 1977), employing a metal-liganding substrate analogue.

From the crystal structure of an enzyme−product complex in the case of the *Pseudomonas* enzyme (Baumann et al., 1993), it could be anticipated that a chelating hydroxamic acid corresponding to the (P_3)-P_2-P_1 portions of our substrates ought to provide a potent competitive inhibitor. Such proved to be the case: Cbz-Leu-Ala-NHOH was prepared and was found to exhibit a K_i value of 40 μM with SMP at neutral pH. Crystallographic investigations have confirmed that the hydroxamate moiety chelatively links to the active-site metal ion in the manner expected (as subsequently depicted). In Figure 4 is shown the pH dependence of pK_i for this inhibitor under k_{cat}/K_m assay conditions ($[S] \ll K_m$). This is an inverse log plot (p$K_i = -\log K_i$), so most effective inhibition corresponds to higher values of pK_i, as seen mid-range. Only the competitive component of inhibition could be examined;

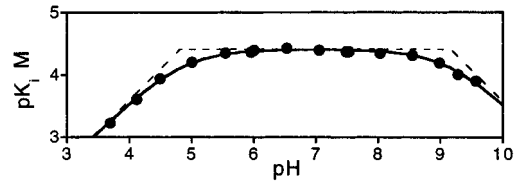

FIGURE 4: Log plot of competitive inhibition constant (pK_i) vs pH for Cbz-Leu-Ala-NHOH and SMP {assay substrates = Txl- and Suc-Phe-Leu-Ala-NH(C_5H_3N)NO_2], [S] $\ll K_m$}. Equation for the fitted line is $(K_i)_{apparent} = (K_i)_{lim}(1 + [H]/K_{a1})(1 + K_{a2}/[H])$. Least-squares fitted parameters are $(K_i)_{lim} = 0.039$ ($\pm$ 0.001) mM, pK_{a1} = 4.81 ($\pm$ 0.02), and pK_{a2} = 9.17 ($\pm$ 0.03). Breaks in dashed-line asymptotes denote pK_a values.

substrate solubility limitations disallowed detection of any concurrent noncompetitive mode.

The salient feature in Figure 4 is that the binding of Cbz-Leu-Ala-NHOH inhibitor is tightest at neutral pH, and enzyme affinity only falls off on the extremes of the profile. According to least-squares curve fitting, there are ionizing groups present having pK_a values of 4.8 and 9.2, which bracket a pH region of firmest liaison between E and I. Of that pair of ionizations, the alkaline-limb pK_a matches that of inhibitor, for deprotonation of its RCONHOH group. Independent spectrophotometric measurement of the hydroxamic acid dissociation in buffered solutions gave a pK_a value of 9.1, which is typical of the functionality. Consequently and not unexpectedly, ionization of that metal-liganding moiety affects inhibition (downturn in pK_i). The enzymic pK_a of ~10 that is seen in k_{cat}/K_m may also influence K_i, but its effect could not be discerned as a practical matter. The acidic-limb pK_a of 4.8 presumably corresponds to an enzymic ionization, and it matches the downturn seen in the k_{cat}/K_m vs pH profile for the Txl substrate. Quite probably that inhibition-perturbing pK_a is due to the same metalloprotein functionality as perceived in catalytic substrate cleavage.

However, a peculiar feature of the pK_i vs pH pattern requires explanation. At neutral pH where binding is tightest, the hydroxamic acid functional group almost certainly yields up a proton upon chelation with the enzymic metal ion. That "acid" only ionizes spontaneously (in the absence of a coordinating metal ion) at pH values of >9, yet chelation of hydroxamic acids to Zn^{2+} is known with certainty to require the deprotonated form within complexes; i.e., the metal ion drives off an H^+ from RCONHOH (Schwarzenbach & Schwarzenbach, 1963; Monzyk & Crumbliss, 1979; Parekh et al., 1989), and hydroxamate *anion* is the species bound (confirmed in this case by inhibitor O to enzyme Zn distances of ~2.1 Å in the E·I crystal structure, subsequently depicted). This would lead to an expectation that binding as a function of aqueous solvent basicity should be proportional to alkali concentration until the pH reaches 9 and should then level off at higher pH values, where the free inhibitor becomes completely ionized and hence available for complexation without competition from protons. Instead, the pH profile is level below 9, and the inhibitor progressively dissociates from enzyme in more alkaline solutions. The unavoidable explanation is that the enzyme must concurrently and obligatorily take up a proton in order for the hydroxamate anion to bind tightly. In that case the implicit cancelation of pH dependences (active enzyme proportional to $[H^+]$, while active inhibitor proportional to $[HO^-]$), yields the level profile actually observed near neutrality. The pK_a of 4.8 noted on the acidic limb of Figure 4 would then correspond

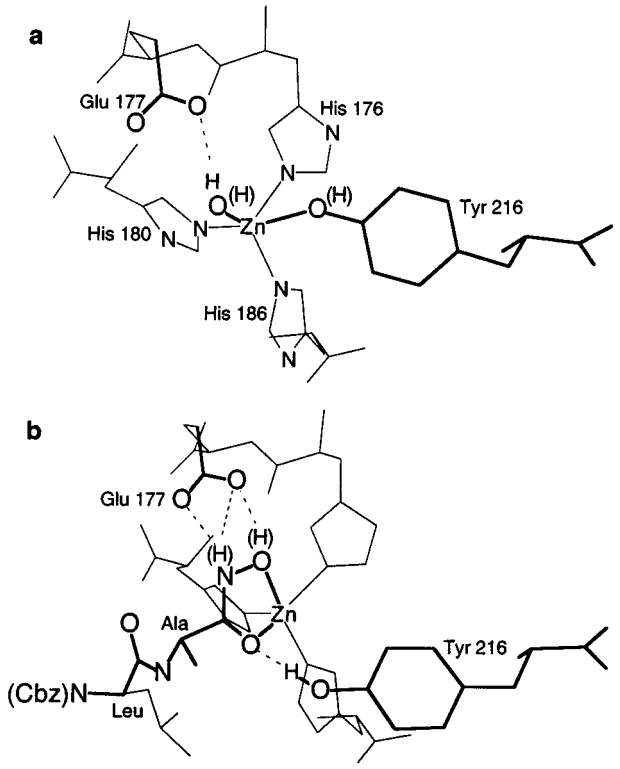

FIGURE 5: Active site of SMP, according to crystallography. (a) Depiction of Zn^{2+} coordination environment for native enzyme (Zn−OAr distance of 2.8 Å). (b) Same with anion of inhibitor Cbz-Leu-Ala-NHOH bound [Zn−OAr distance of 4.2 Å, hydroxamate-to-zinc distances of 2.12 Å (Zn−O_N) and 2.07 Å (Zn−O_C)]. Enzymic tyrosine may H-bond to the hydroxamic imidate oxygen of inhibitor [(H)ON=C(R)O^- to O(H)Ar distance of 2.7 Å], and inhibitor appears to H-bond to the side-chain carboxylate of Glu 177 [$RCOO^-$ to O(H)N(H)C(OZn)R distances of 2.5−3.3 Å]. Other E·I contacts are mentioned in the Materials and Methods section (structure provided courtesy of U. Baumann).

to the critical proton-accepting enzymic functional group, which must adopt its *conjugate acid form* in order for hydroxamate *anion* to bind tightly, at all pH values ("reverse protonation" inhibition: Mock & Tsay, 1986, 1988; Mock et al., 1993; Mock & Aksamawati, 1994).

In order to identify the latter moiety, it is appropriate to consult the enzyme crystal structure, a portion of which is shown in Figure 5. Although protons cannot actually be seen crystallographically, one evident candidate for the pK_a of 4.8 would be the side chain of a glutamic acid residue from the enzyme, Glu 177, which prominently dwells in the vicinity of the active-site metal ion. This residue has a prevalent counterpart in most other metalloproteases. Furthermore, the -$CH_2CH_2CO_2$(H) moiety appears to become involved in H-bonding with the bound hydroxamate (Figure 5b). However, that side chain is unlikely to be responsible for controlling inhibitor binding in the manner described, because of obligatory participation by the enzyme in its conjugate acid form only. In order to explain the observed pH profile for pK_i employing Glu 177 as the regulatory species, it would be necessary that presence of the *deprotonated* form of the carboxyl residue (Glu 177-CO_2^-) should induce complete rejection of the inhibitor by enzyme. Because no compensatory inflection may be seen in the pK_i vs pH profile at any pH up to 10, the putative conjugate acid Glu 177-CO_2H within the E·I complex would be obliged to have a pK_a value of >10 so long as the inhibitor is bound.

Scheme 2

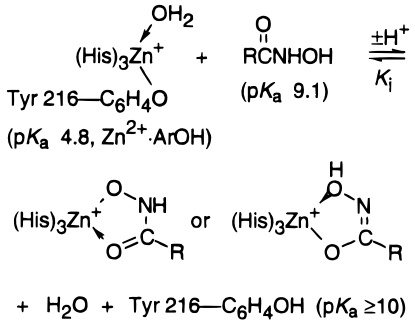

That is a thermodynamic imperative attending any provisional stipulation that the carboxylate anion absolutely prevents inhibitor binding, which the pH profile seems to require. Such an extreme pK_a perturbation of an enzymic carboxylic acid upon binding of a reactant analogue is improbable. It cannot readily be attributed to introduction of a new H-bond, since apparently similar carboxylate H-bonding to $H_2O{\cdot}Zn^{2+}$ occurs in the absence of inhibitor (Figure 5a). Furthermore, if a substantial pK_a perturbation of Glu 177 were being induced by the presence of Cbz-Leu-Ala-NHOH, then a quenching of glutamic acid side-chain acidity should also take place with peptide substrates as well, meaning that this particular active-site carboxylate functionality on the enzyme would be unavailable as an anion for catalytic purposes within E·S complexes.

A more reasonable explanation of the pK_i vs pH profile is that one of the active-site metal ligands present in the uncomplexed enzyme is responsible for the acidic limb. Examination of protein crystal structures indicates that the Zn^{2+} is held in place by three histidine residues, as shown in Figure 5a. The zinc also bears a solvent (H_2O) ligand, and additionally the phenolic hydroxyl of residue Tyr 216 appears to ligate to the metal ion in the free enzyme, at an apical position within the latter's trigonal-bipyramidal coordination sphere, although that side chain moves away when the active site becomes filled with a substrate analogue such as the hydroxamate inhibitor [Figure 5b; also compare Baumann et al. (1993), Miyatake et al. (1995), and Grams et al. (1996)]. We suggest that the pK_a of 4.8 is most plausibly attributed to that ArOH residue, in that a phenol possesses the greatest intrinsic acidity of the five metal ligands. Association of the phenolic hydroxyl (nominal pK_a of ~10) with a Lewis acid such as Zn^{2+} most certainly would further acidify the OH, and a 5 pK-unit perturbation is not unreasonable. Because the enzymic *phenolate anion* thereby provided (Tyr-ArO^-) apparently cannot be displaced from Zn^{2+} by prevailing concentrations of external hydroxamate, the experimental requirement of proton uptake by the enzyme for effective inhibition is accommodated ($ArO^- \rightarrow ArOH$). This explanation, summarized in Scheme 2, constitutes the most satisfactory rationalization of the pH dependence of K_i for SMP complexing with the hydroxamic acid inhibitor Cbz-Leu-Ala-NHOH.

Some qualifications must be attached to this explanation. Because in Figure 5a the $Zn-OH_2$ interatomic distance (1.9 Å) is shorter than the $Zn-O^-Ar$ distance (2.8 Å), the occurrence of a ligand tautomerism must be allowed: $H_2O{\cdot}Zn^+-OAr \rightleftharpoons HO-Zn^+{\cdot}HOAr$; i.e., the macroscopic deprotonation actually observed in inhibitor binding could arise in part from both Zn−water and Zn−phenol, despite a phenol being the intrinsically more acidic constituent. A suggested H-bond involving the active-site carboxylate, Glu 177$-CO_2^-\cdots H_2O{\cdot}Zn^+$ (O−O distance 2.8 Å, Figure 5a), ought to promote the zinc−phenolate tautomer. Such a proton redistribution does not materially affect the inhibitor binding explanation, in that both zinc−oxygen ligands in Figure 5a are displaced when hydroxamate chelates to Zn^{2+}. Likewise, either half of the equilibrium could constitute the catalytically active species, with indistinguishable kinetic consequences, regardless of which tautomer is actually favored thermodynamically (see Discussion). In addition to that consideration, a question arises as to which tautomer of the hydroxamate anion may be present within the E·I complex (Scheme 2). The interatomic distance from Glu 177$-CO_2^-$ to the hydroxylamide oxygen (2.5 Å) appears shorter than to the hydroxylamide nitrogen (3 Å), with proper allowance for limited resolution within the crystallographic structure determination (Figure 5b). Presence of a Glu 177-$CO_2^{(-)}\cdots H^+\cdots{}^{(-)}$ON(H)COR linkage would imply either that the HON═C(O^-)R tautomer predominates in the complex or that Glu 177 is in fact present as a carboxyl group, H-bonding to the chelated $^-$ONHC(═O)R tautomer.[3] As was previously described, on account of the pH profile in Figure 4 the latter interpretation is disfavored, because it necessitates that the pK_a of that RCO_2H be perturbed from a value of <5 to one of >10 upon inhibitor complexation, and it also would carry the implication that neither $H_2O{\cdot}Zn^{2+}$ nor $ArOH{\cdot}Zn^{2+}$ in the uncomplexed enzyme has a pK_a of <10 (since deprotonation of either of those moieties most certainly should perturb pK_i for Cbz-Leu-Ala-NHOH). The pattern of H-bonding here is similar to that found in hydroxamate inhibitor complexes of thermolysin (Holmes & Matthews, 1981), which association exhibits a similar pH dependence for K_i (Izquierdo-Martin & Stein, 1992), and which requires a similar explanation (Mock & Aksamawati, 1994).

DISCUSSION

Conventional mechanistic thinking for catalysis by metalloproteases has employed the carboxylate side chain present at the active site (Glu 177 in the present case) to function as an essential general base. It supposedly aids concerted migration, onto an incipiently metal-bound substrate carboxamide, of an H_2O addend that was initially affixed to the active-site Zn^{2+} (Matthews, 1988). However, recent kinetic evidence obtained for thermolysin, the enzyme for which that mechanism was devised, has forced a major revision of this interpretation (Mock & Aksamawati, 1994; Mock & Stanford, 1996). The present investigation was undertaken to see if the revamped mechanism as deduced for thermolysin could be reconciled with the existence of metalloproteases lacking the catalytic active-site histidine present in that enzyme, which residue appears to engage in a more consequential mechanistic role than previously appreciated [see also Mock and Xu (1994) for carboxypeptidase A catalysis].

[3] The $^-$ONHC(═O)R tautomer is usually considered to be the metal-binding species, but the HON═C(O^-)R tautomer is favored upon hydroxamic acid ionization in the absence of chelation (Bauer & Exner, 1974; Steinberg & Swidler, 1990; Decouzon et al., 1990; Bordwell et al., 1990). Either tautomer could be present in the E·I complex, and Zn-to-O distances are equivalent in the crystal structure, giving no basis for preference.

Scheme 3

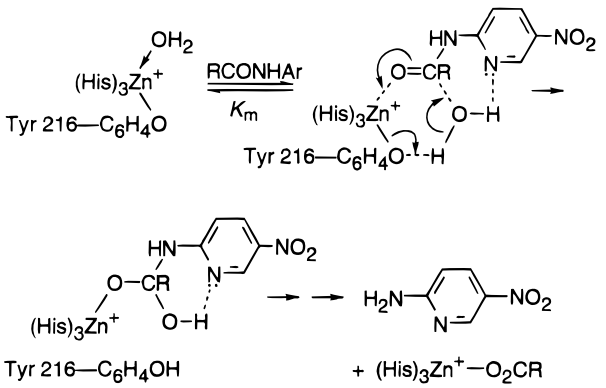

Peptidolytic Mechanism for Serralysins. The proffered explanation in the previous section as regards competitive hydroxamate inhibitor binding to serralysin has relevance for the catalytic mechanism of substrate hydrolysis. Analogously to the *equilibrium binding* behavior for K_i shown in Figure 4, it was found *kinetically* that the specificity constant k_{cat}/K_m also exhibits an essentially level pH dependence between the extremes of pH 5 and 10, as is most clearly exemplified with substrate Txl-Phe-Leu-Ala-NH(C_5H_3N)-NO_2, and that pattern apparently holds true for k_{cat} as well (Figures 2 and 3, log plots in each case). However, no plausible ionization comparable to that of a hydroxamic acid, occurring on the substrate and accompanying productive binding, can be identified.[4] Consequently, either the pK_i-regulating phenolate of Tyr 216 (provisionally deemed the active tautomer for simplicity) remains ligated as such to the metal ion throughout catalysis, which seems unlikely (due to its Lewis acidity-quenching effect upon Zn^{2+} and because of its crystallographically observed displacement in various peptide-type complexes of SMP, AP, and related proteases; Baumann et al., 1993, 1995; Gomis-Rüth et al., 1993; Miyatake et al., 1995) or the ligand becomes released only in the course of the catalytic reaction. Since the phenolate of that residue would have to take up a proton in order to dissociate from the Zn^{2+}, assignment of that ArO^- residue to a general base role in the course of catalysis suggests itself.

A plausible chemical mechanism for substrate conversion is depicted in Scheme 3. In a first step, substrate scissile -CONH- reversibly displaces the H_2O molecule that is initially coordinated to Zn^{2+} (active tautomer) according to Figure 5a, with the latter metal ion held to the enzyme by the three His imidazoles and the one phenolate (Tyr 216-ArO^-). Because a carboxamide oxygen atom and an ordinary water molecule are comparably basic (pK_a values of -1 to -1.7 for conjugate-acid forms), such an exchange should be feasible without thermodynamic penalty. Due to the concomitant dative linkage by an enzymic phenoxide directed toward the active-site Zn^{2+}, the departing H_2O should be sufficiently labile to equilibrate with bulk solvent *via* this substitution. According to Scheme 3 the Tyr 216 phenolate group, tenuously metal-ligated at the incept, functions subsequently within the E·S complex as a general base to deprotonate a solvent water-molecule nucleophile, as the latter attacks the zinc-activated substrate, with the ArOH being released from zinc contemporaneously with creation of a *gem*-diolate tetrahedral adduct of the scissile carboxamide on the active-site metal ion. Again, the basicity of a phenolate and that of an amido tetrahedral-adduct anion are comparable (Satterthwait & Jencks, 1974a,b), so the proposed transformation should not encounter a thermodynamic barrier on that score. Contraction of the valence shell of the zinc ion to tetracoordinate as shown enhances the latter's Lewis acidity (Kimura & Koike, 1991; Sigel & Martin, 1994), providing crucial stabilization for the transient oxyanionic tetrahedral-adduct intermediate, which is a cardinal feature of metalloprotease mechanisms (Mock et al., 1993). In this mechanism the actual H_2O-nucleophile addend is *not* required to be that specific water molecule initially attached to Zn^{2+} [see Mock and Stanford (1996) for reasons disfavoring the latter concept].

Important to the mechanistic argument of Scheme 3 is a realization that the Tyr 216 phenolate should be insecurely bound (apically) to the pentacoordinate Zn^{2+} in the unoccupied enzyme. That is indicated by the Zn−OAr interatomic distance (2.8 Å) and by the relatively small phenolic pK_a perturbation of 5 units (indicating a $ArO^-\cdot Zn^{2+}$ virtual association energy of $\Delta G \sim 5.5$ kcal/mol, comparable to a strong H-bond). In contrast, an H_2O acidified by tetracoordinate Zn^{2+} may experience a ∼10-unit shift in pK_a (Kimura & Koike, 1991; Sigel & Martin, 1994; Mock & Tsay, 1986, 1988; Mock et al., 1993; Mock & Aksamawati, 1994), and the Zn−OAr interatomic distance in a phenolate-containing inhibitor so bound to carboxypeptidase A has been reported as 2.0 Å (Feinberg et al., 1995). Hence, the phenolate anion of Tyr 216 in serralysin becomes entirely available mechanistically, *via* the metal ion, to function as a general base at pH values of >5. Its intrinsic proton affinity reemerges when ArO^- releases from Zn^{2+} as depicted. In Scheme 3 the H_2O nucleophile is also shown hydrogen-bonding to the pyridine nitrogen of the leaving amine. The latter is suggested by molecular modeling of the reaction course and may in part account for the observation that the corresponding *p*-nitroanilide, without such an H-bond acceptor, is inefficiently cleaved. Structural modeling suggests that a comparable H-bond is directed to the amide carbonyl oxygen of the P_1' residue in the case of normal peptide substrates, so this could be a regular specificity feature, although at present that is speculative. In completion of this catalytic mechanism, rapid subsequent breakdown of the *gem*-diolate tetrahedral adduct ensues, yielding a Zn-carboxylate and the amine component of the scissile linkage (with requisite proton transfers again possibly mediated by the tyrosine).

In the proposed scheme the prominent enzyme glutamate side chain at the active site (Glu 177-CO_2^-), the presence of which seems to be a generic feature of metalloproteases, is not called upon to play an active catalytic role (acid−base or nucleophilic). This is in accord with present understanding of the proteolytic mechanism for thermolysin, where the corresponding enzymic carboxylate evidently serves merely as an anion, passively providing electrostatic stabilization to electron-deficient intermediates created in proximity during the catalytic cycle (Mock & Stanford, 1996). The enzymic glutamate in serralysin may also transiently H-bond to the scissile carboxamide NH, indirectly facilitating release of Tyr 216 phenoxide from zinc by further

[4] The nitropyridinamide moiety yields an anion at pH > 11 (N-H ionization), but that species should be inert to catalytic hydrolysis (by any mechanism involving carbonyl hydration). The corresponding pK_a for a normal peptide substrate would be ≥15.

polarizing the −C(═O)NH− group marginally. In at least one metalloprotease that intact glutamate has been found inessential by mutational evidence (Glu → Asp; Windsor et al., 1994). For the mechanistically affiliated zinc protease thermolysin, an enzymic imidazole participating in a catalytic process similar to Scheme 3 serves as the proton acceptor (His 231 of thermolysin, correspondingly situated relative to the reaction center as is Tyr 216, but never metal-coordinated), providing general-base assistance to hydration of the Zn^{2+}-activated substrate carboxamide (Mock & Stanford, 1996). Evidently in the serralysins that role has devolved to the phenolate side chain of a tyrosine residue. The accrued catalytic advantage for the latter proteases appears to be a broader pH range of enzymic activity, extending well into the alkaline region.

It is worth observing that Tyr 216 ultimately reenters into ligation with the serralysin Zn^{2+}, once the carboxylate group produced from substrate by catalysis has departed from the active site. Because product release frequently becomes rate-limiting in enzymic reactions, the presence of an internal displacing ligand for that step may constitute an additional reason for proximity of the tyrosine residue to the metal ion.

The general features of the catalytic pH profiles are then explained as follows (k_{cat}/K_m, Txl substrate). Loss of activity in acidic solution corresponds to protonation of the anionic Tyr 216 side chain ($ArOH{\cdot}Zn^{2+} \rightarrow ArOZn^{+} + H^{+}$, p$K_a$ of 4.8). That quenches the general-base catalysis required in Scheme 3, and the ionization shows up in k_{cat} as would be expected (Figure 3). This acidic-limb pK_a assignment actually derives from the pH dependence of hydroxamate-inhibitor binding, an autonomous *equilibrium*, and so is not contingent on the proposed *kinetic* mechanism of substrate conversion. In this connection, acknowledgement should again be given of possible tautomeric equilibrium within the enzyme, $H_2O{\cdot}Zn^{+}-OAr$ (Tyr 216) ⇌ $HO-Zn^{+}{\cdot}HOAr$ (Tyr 216). So long as the prototopic shift is facile, the phenoxide form can perform as the catalytically active species, even should it be a thermodynamically disfavored tautomer within the enzyme prior to substrate complexation. On the alkaline limb of the pH profile, deprotonation of some other enzymic group (pK_a of ∼10) also prevents catalysis. Although this need not be an active-site residue, particular attention is drawn to the three histidines that serve to bind the essential Zn^{2+}. Previous model studies have shown that coordination of a transition metal ion to one of the nitrogens of an imidazole ring *acidifies* the other heterocycle NH to a pK_a of 9−11 (Sundberg & Martin, 1974). That value is sensibly intermediate between the first and second acid dissociation constants of imidazolium ion, for which pK_a values are 7 and 14. The suggested perturbation of imidazole acidity in the present case (ΔpK_a of ∼4 units) is comparable to that proposed for the phenolic zinc ligand of SMP and AP. Such an imidazole deprotonation at the enzymic active site would markedly suppress the Lewis acidity of the metal ion (a coordinated imidazolate being a much stronger electron donor), and that could in turn preclude catalytically necessary activation of the substrate. Alternatively, the zinc-bound water molecule that substrate is obliged to substitute in the course of ligation (Scheme 3, K_m step) could become completely converted to an undisplaceable Zn^{2+}-hydroxide at that pH (e.g., HO−Zn−OAr). These possibilities are summarized in Scheme 4. The small upward inflection on the rate profile near pH 5−6 that is seen with the serralysin

Scheme 4

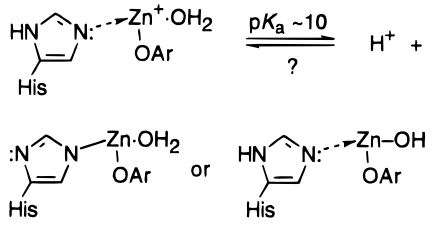

proteases and the Txl substrate correlates experimentally with a slow activation of SMP for our substrates in that region. That slight hump on the acidic limb of the upper profiles in Figures 2 and 3 requires that some enzymic functional group other than Tyr 216, but with a similar pK_a, perturbs the rate constants by a factor of ∼6. Such behavior could actually have a remote origin, but speculation about subtle pH-dependent enzymic conformational shifts, etc., is presently unwarranted for what is in fact a minor kinetic disturbance.[5]

Conclusion. It has become clear that no single, universal chemical mechanism suffices to explain metalloprotease catalysis. Thermolysin uses a reverse-protonation pathway involving Zn-Lewis acid activation of substrate, plus subsequent histidine general-base participation (Mock & Stanford, 1996). A number of aminopeptidases engage two active-site metal ions in concert to cleave their substrates (Mock & Liu, 1995). As here shown, the serralysins appear to employ yet another variation. The one unifying enzyme feature appears to be an especially Lewis-acidic zinc ion, for which the main catalytic function is to stabilize the tetrahedral-adduct oxyanion generated by hydroxide addition to the Zn^{2+}-activated scissile carboxamide linkage (Mock et al., 1993). In the various zinc proteases delivery of that HO^{-} nucleophile to substrate may occur from a second metal ion (as in dual-metal aminopeptidases; Mock & Liu, 1995), or may be facilitated by general-base catalysis upon a solvent H_2O by an appropriately situated enzymic imidazole (as in thermolysin; Mock & Stanford, 1996), or may be aided intramolecularly in the same fashion by a substrate carboxylate group (as in carboxypeptidase A; Mock & Zhang, 1991; Mock & Xu, 1994). Or, in the case of metalloproteases that need to operate at high pH, an HO^{-} nucleophile may be supplied *via* the aqueous medium and a phenolate base that is initially engaged with the metal ion (as here suggested for serralysins). The latter mechanism, which was sum-

[5] It should be acknowledged that the conventional explanation of metalloprotease catalysis, in which an H_2O initially coordinated to Zn^{2+} concertedly migrates to the scissile amide carbonyl with the aid of a glutamic acid residue (a formulation which was found unsatisfactory for thermolysin; Mock & Stanford, 1996), is not excluded by present evidence for serralysin. However, should the kinetically observed acidic-limb pK_a of ∼4.8 be attributed to Glu 177-CO_2^{-} operating as a base, then the pK_a of active-site $Zn^{2+}{\cdot}OH_2$ (or $Zn^{2+}{\cdot}OHAr$) must be ≥10 according to the pH−rate profiles (which show no break at a lower pH). That would imply diminished rather than enhanced Lewis acidity of the enzymic zinc ion [relative to uncomplexed $(H_2O)_n{\cdot}Zn^{2+}$, pK_a ∼ 9] and so does not as adequately explain stabilization of the tetrahedral-adduct intermediate that occurs during catalysis (Mock et al., 1993). Also, an apparent contradiction arises in the conjugate *acid* form of the pK_a of ∼4.8 residue being absolutely required for substrate-analogue inhibitor binding (Figure 4), but the conjugate *base* form of the same residue being needed for chemical conversion of enzyme-bound substrate (Figures 2 and 3). That conflict is resolved by attribution of the pK_a of 4.8 to Tyr 216 in coordination with Zn^{2+}.

[6] Certain of the metzincins (adamalysins and some collagenases) lack the Tyr 216 residue at their active sites. It is essential that they be subjected to comparable kinetic investigations.

marized in Scheme 3, will require additional substantiation. The transformation of substrate to tetrahedral adduct has been formulated rudimentarily as a concerted chemical process, but serial-stepwise variations for the same general pathway are possible and would perhaps be theoretically preferable.[6] In the longer view, there is reason to hope that the catalytic differences occurring among the various kinds of metalloproteases can be exploited to design inactivators that work selectively upon but one type, a possibility with practical consequences as regards pharmaceutical design for the many proteolytic zinc enzymes of biomedical importance.

ACKNOWLEDGMENT

We thank Dr. Jiu-Tsair Tsay for some preliminary kinetic measurements and Dr. Ulrich Baumann for permission to use the E·I crystal structure prior to publication.

REFERENCES

Bauer, L., & Exner, O. (1974) *Angew. Chem., Int. Ed. Engl. 13*, 376−384.
Baumann, U. (1994) *J. Mol. Biol. 242*, 244−251.
Baumann, U., Wu, S., Flaherty, K. M., & McKay, D. B. (1993) *EMBO J. 12*, 3357−3364.
Baumann, U., Bauer, M., Létoffé, S., Delepelaire, P., & Wandersman, C. (1995) *J. Mol. Biol. 248*, 653−661.
Bond, J. S., & Beynon, R. J. (1995) *Protein Sci. 4*, 1247−1261.
Bordwell, F. G., Fried, H. E., Hughes, D. L., Lynch, T.-Y., Satish, A. V., & Whang, Y. E. (1990) *J. Org. Chem. 55*, 3330−3336.
Cleland, W. W. (1977) *Adv. Enzymol. Relat. Areas Mol. Biol. 45*, 273−387.
Decouzon, M., Exner, O., Gal, J.-F., & Maria, P.-C. (1990) *J. Org. Chem. 55*, 3980−3981.
Erlanger, B. F., Kokowsky, N., & Cohen, W. (1961) *Arch. Biochem. Biophys. 95*, 271−278.
Feinberg, H., Greenblatt, H. M., Behar, V., Gilon, C., Cohen, S., Bino, A., & Shoham, G. (1995) *Acta Crystallogr. D51*, 428−449.
Gomis-Rüth, F. X., Stöcker, W., Huber, R., Zwilling, R., & Bode, W. (1993) *J. Mol. Biol. 229*, 945−968.
Grams, F., Dive, V., Yiotakis, A., Yiallouros, I., Vassiliou, S., Zwilling, R., Bode, W. & Stöcker, W. (1996) *Nat. Struct. Biol. 3*, 671−675.
Hamada, K., Hata, Y., Katsuya, Y., Hiramatsu, H., Fujiwara, T., & Katsube, Y. (1996) *J. Biochem. (Tokyo) 119*, 844−851.
Holmes, M. A., & Matthews, B. W. (1981) *Biochemistry 20*, 6912−6920.
Hooper, N. M. (1994) *FEBS Lett. 354*, 1−6.
Izquierdo-Martin, M., & Stein, R. L. (1992) *J. Am. Chem. Soc. 114*, 325−331.
Jiang, W., & Bond, J. S. (1992) *FEBS Lett. 312*, 110−114.
Kimura, E., & Koike, T. (1991) *Comments Inorg. Chem. 11*, 285−301.
Matthews, B. W. (1988) *Acc. Chem. Res. 21*, 333−340.
Miyata, K., Maejima, K., Tomoda, K., & Isono, M. (1970a) *Agric. Biol. Chem. 34*, 310−318.
Miyata, K., Tomoda, K., & Isono, M. (1970b) *Agric. Biol. Chem. 35*, 460−467.
Miyata, K., Tomoda, K., & Isono, M. (1970c) *Agric. Biol. Chem. 34*, 1457−1462.
Miyatake, H., Hata, Y., Fujii, T., Hamada, K., Morihara, K., & Katsube, Y. (1995) *J. Biochem. (Tokyo) 118*, 474−479.
Mock, W. L., & Tsay, J.-T. (1986) *Biochemistry 25*, 2920−2927.
Mock, W. L., & Tsay, J.-T. (1988) *J. Biol. Chem. 263*, 8635−8641.
Mock, W. L., & Zhang, J. Z. (1991) *J. Biol. Chem. 266*, 6393−6400.
Mock, W. L., & Aksamawati, M. (1994) *Biochem. J. 302*, 57−68.
Mock, W. L., & Xu, X. (1994) *Bioorg. Chem. 22*, 373−386.
Mock, W. L., & Liu, Y. (1995) *J. Biol. Chem. 270*, 18437−18446.
Mock, W. L., & Stanford, D. L. (1996) *Biochemistry 35*, 7369−7377.
Mock, W. L., Freeman, D. J., & Aksamawati, M. (1993) *Biochem. J. 289*, 185−193.
Monzyk, B., & Crumbliss, A. L. (1979) *J. Am. Chem. Soc. 101*, 6203−6213.
Morihara, K. (1963) *Biochim. Biophys. Acta 73*, 113−124.
Morihara, K., Tsuzuki, H., & Oka, Y. (1973) *Biochim. Biophys. Acta 309*, 414−429.
Nakahama, K., Yoshimura, K., Marumoto, R., Kikuchi, M., Lee, I. S., Hase, T., & Matsubara, H. (1986) *Nucleic Acids Res. 14*, 5843−5855.
Parekh, P. C., Manon, S. K., & Agrawal, Y. K. (1989) *J. Chem. Soc., Perkin Trans. 2*, 1117−1123.
Rawlings, N. D., & Barrett, A. J. (1995) *Methods Enzymol. 248*, 183−228.
Satterthwait, A. C., & Jencks, W. P. (1974a) *J. Am. Chem. Soc. 96*, 7018−7031.
Satterthwait, A. C., & Jencks, W. P. (1974b) *J. Am. Chem. Soc. 96*, 7031−7044.
Schechter, I., & Berger, A. (1967) *Biochem. Biophys. Res. Commun. 27*, 157−162.
Schwarzenbach, G., & Schwarzenbach, K. (1963) *Helv. Chim. Acta 46*, 1390−1400.
Sigel, H., & Martin, R. B. (1994) *Chem. Soc. Rev. 23*, 83−91.
Steinberg, G. M., & Swidler, R. (1990) *J. Org. Chem. 30*, 2362−2365.
Stöcker, W., & Bode, W. (1995) *Curr. Opin. Struct. Biol. 5*, 383−390.
Stöcker, W., Grams, F., Baumann, U., Reinemer, P., Gomis-Rüth, F. X., McKay, D. B., & Bode, W. (1995) *Protein Sci. 4*, 823−840.
Sundberg, R. J., & Martin, R. B. (1974) *Chem. Rev. 74*, 471−517.
Windsor, L. J., Bodden, M. K., Birkedal-Hansen, B., Engler, J. A., & Birkedal-Hansen, H. (1994) *J. Biol. Chem. 269*, 26201−26207.
Wolz, R. L. (1994) *Arch. Biochem. Biophys. 310*, 144−151.

BI963149P